GPR3 expression in retinal ganglion cells contributes to neuron survival and accelerates axonal regeneration after optic nerve crush in mice

Shun Masuda[1, 2], Shigeru Tanaka[1]*, Hiroko Shiraki[1], Yusuke Sotomaru[3], Kana Harada[1], Izumi Hide[1], Yoshiaki Kiuchi[2], Norio Sakai[1]

[1)] Department of Molecular and Pharmacological Neuroscience and [2)] Department of Ophthalmology, Graduate School of Biomedical and Health Sciences; [3)] Natural Science Center for Basic Research and Development, Hiroshima University
1-2-3 Kasumi, Minami-ku, Hiroshima 734-8551, Japan

*Address correspondence to: Shigeru Tanaka
Department of Molecular and Pharmacological Neuroscience
Graduate School of Biomedical and Health Sciences, Hiroshima University
1-2-3 Kasumi, Minami-ku, Hiroshima 734-8551, Japan
Email: tanakamd@hiroshima-u.ac.jp

Abstract

Glaucoma is an optic neuropathy and is currently one of the most common diseases that leads to irreversible blindness. The axonal degeneration that occurs before retinal ganglion neuronal loss is suggested to be involved in the pathogenesis of glaucoma. G protein-coupled receptor 3 (GPR3) belongs to the class A rhodopsin-type GPCR family and is highly expressed in various neurons. GPR3 is unique in its ability to constitutively activate the Gαs protein without a ligand, which elevates the basal intracellular cAMP level. Our earlier reports suggested that GPR3 enhances both neurite outgrowth and neuronal survival. However, the potential role of GPR3 in axonal regeneration after neuronal injury has not been elucidated. Herein, we investigated retinal GPR3 expression and its possible involvement in axonal regeneration after retinal injury in mice. GPR3 was relatively highly expressed in retinal ganglion cells (RGCs). Surprisingly, RGCs in GPR3 knockout mice were vulnerable to neural death during aging without affecting high intraocular pressure (IOP) and under ischemic conditions. Primary cultured neurons from the retina showed that GPR3 expression was correlated with neurite outgrowth and neuronal survival. Evaluation of the effect of GPR3 on axonal regeneration using GPR3 knockout mice revealed that GPR3 in RGCs participates in axonal regeneration after optic nerve crush (ONC) under zymosan stimulation. In addition, regenerating axons were further stimulated when GPR3 was upregulated in RGCs, and the effect was further augmented when combined with zymosan treatment. These results suggest that GPR3 expression in RGCs helps maintain neuronal survival and accelerates axonal regeneration after ONC in mice.

Keywords: GPR3, cAMP, axonal regeneration, retinal granular cells, neuronal survival, optic nerve injury, glaucoma.

Introduction

Glaucoma is an optic neuropathy that affects more than 60 million people worldwide and is currently one of the most common diseases that leads to irreversible blindness (Quigley, 2011). Loss of RGCs because of high IOP is related to the progression of glaucoma pathogenesis; however, loss of RGCs sometimes occurs in patients with normal IOP, which is called normal tension glaucoma (NTG) (Mallick et al., 2016; Weinreb et al., 2014).

Optic neuropathy associated with glaucoma is related to multiple factors. In addition to high IOP, these factors include aging (Luu and Palczewski, 2018), systemic hypotension (Promelle et al., 2016), oxidative stress (Bonne et al., 1998; Gherghel et al., 2013), glutamatergic neurotoxicity (Seki and Lipton, 2008), increased levels of nitric oxide (Cavet et al., 2014), decreased levels of trophic factors (Gupta et al., 2014), and genetic factors (including optineurin and myocilin) (Weisschuh et al., 2005; Weisschuh et al., 2007). Pharmacological treatment of glaucoma has been limited to IOP-lowering agents; therefore, novel drugs protecting RGNs from these harmful factors are being developed. For example, neurotrophic factors (including CNTF, BDNF, NGF, and VGF) (Lambuk et al., 2022), an anti-inflammatory drug (1α,25-dihydroxyvitamin D_3) (Lazzara et al., 2021), and a P2X7 receptor antagonist (Platania et al., 2022; Romano et al., 2020) have been considered for glaucoma treatment. To accelerate drug development for glaucoma, it is essential to investigate the pathophysiology and molecular mechanisms underlining glaucoma. However, the molecular mechanisms of glaucoma, especially for NTG, have not been fully elucidated.

Meanwhile, axon dysfunction and degeneration are observed before the number of RGCs decreases in a mouse model of glaucoma (Buckingham et al., 2008). Neuronal loss is caused by downregulation of intracellular cAMP after injury, which in turn decreases the responsiveness of specific neurotrophic factors such as BDNF and IGF1, thereby leading to RGC death (Cui et al., 2003; Shen et al., 1999). Interestingly, responsiveness to neurotrophic factors is restored when neurons are treated with depolarizing stimuli or by pharmacological activation of intracellular cAMP (Meyer-Franke et al., 1998). cAMP is a key regulator of neuronal survival and axon growth in neurons and plays a diverse role in axonal regeneration (Stiles et al., 2014). In addition, elevation of cAMP stimulates expression of neurotrophins, such as BDNF and CNTF, via a calcium-dependent mechanism, which promotes neuronal survival in a MAPK- and phosphoinositide 3-kinase (PI3K)-dependent manner (Finkbeiner and Greenberg, 1998; Tao et al., 1998). Moreover, cAMP elevation in neurons also stimulates neurite outgrowth and protects against myelin-associated inhibitory factors (Gao et al., 2003; Kao et al., 2002). Meanwhile, optic nerve regeneration after axonal injury could be partially achieved by intraocular inflammation (i.e., mechanical injury or the Toll-like receptor 2 ligand zymosan) and its downstream effectors (i.e., oncomodulin), transcription factors (i.e., Kif), trophic factors and chemokines(i.e., CCL5), and cell-intrinsic suppressors of axonal regeneration (i.e., suppressor of cytokine signaling 3 (SOCS3) and phosphatase and tensin homolog (PTEN) inhibitors) (Benowitz et al., 2017; Xie et al., 2021). Interestingly, several reports have suggested that axonal regeneration induced by zymosan, oncomodulin, or neurotrophic factors could be augmented by cAMP elevation via of chlorophenylthio-cAMP (CPT-

cAMP) administration (Cui et al., 2003; Kurimoto et al., 2010; Park et al., 2004; Yin et al., 2006). Therefore, intracellular cAMP elevation has a multimodal effect on neuronal survival and neuronal outgrowth and is suggested to be important for neuronal regeneration after axonal injury.

G protein-coupled receptor 3 (GPR3) is a member of the class A rhodopsin-type GPCR family and is highly expressed in various neurons (Ikawa et al., 2021; Saeki et al., 1993). A unique feature of GPR3 is its constitutive activation of the Gαs protein without a ligand, which increases the basal intracellular cAMP level (Eggerickx et al., 1995; Sveidahl Johansen et al., 2021). In cerebellar granular neurons (CGNs), GPR3 expression increases during neuronal development, both in vitro and in vivo, and stimulates neurite outgrowth and neuronal survival in response to various apoptosis-inducing stimuli, including ischemia, in a PI3K- and MAPK-dependent manner (Tanaka et al., 2007; Tanaka et al., 2014; Tanaka et al., 2021). Furthermore, in cultured CGNs, GPR3 and its subfamily of receptors can promote neurite outgrowth and resist myelin-associated glycoprotein inhibition (Tanaka et al., 2007). Moreover, GPR3 expression is sustained throughout the lifespan in various neurons of the CNS (Ikawa et al., 2021) and protects neurons under ischemic conditions (Tanaka et al., 2014). However, the physiological roles of GPR3 in neuronal survival and axonal regeneration in vivo have not been elucidated.

In the present study, we identified GPR3 expression in mouse RGCs. Surprisingly, the number of RGCs was significantly reduced in GPR3 knockout mice compared with wild-type mice as early as 10 weeks of age, despite mice having normal IOP. We further

explored the possible involvement of GPR3 in RGC survival after retinal ischemia and axonal regeneration after optic nerve crush (ONC) in mice.

Materials and methods

Animals

All investigations were performed in accordance with the Association for Research in Vision and Ophthalmology Statement for the Use of Animals in Ophthalmic and Vision Research, and all experiments were approved by the Animal Care and Use Committee of Hiroshima University (approval numbers 25-193-3, 25-194-4, 30-153, and 30-154). GPR3 knockout mice with a B6 background were acquired from MMRRC (Bar Harbor, ME, USA) as cryopreserved embryos and were manipulated and implanted at the Institute of Laboratory Animal Science, Hiroshima University, as previously reported (Tanaka et al., 2014). Experiments were performed with male C57BL/6j mice aged 8–10 weeks (Japan SLC, Inc., Hamamatsu, Japan) unless otherwise indicated.

Generation of PA-GPR3 knockin mice

We generated PA-GPR3 knockin mice using the CRISPR-Cas9 genome editing system (Li et al., 2013). Single-stranded oligodeoxynucleotides (ssODNs), including the PA-tag sequence "GCCTGCCAGCATCTCATAGGACCTTTCTTCTACAGGTACCGGATCCATGGGCGT TGCCATGCCAGGTGCCGAAGATGATGTGGTGTGGGGAGCAGGAAGCTCTATGGC CTGGTTCTCAGCTGGCT" and crRNA "CTTCTACAGGTACCATGATGTGG", were synthesized by Integrated DNA Technologies (IDT, Coralville, IA, USA). Alt-R Sp Cas9 Nuclease HiFi 3NLS Cas9 enzyme and ATTO550-labeled tracrRNA were also purchased from IDT. The crRNA-tracrRNA complex was first prepared, followed by mixing of Cas9

enzyme, crRNA-tracrRNA, and ssODNs at final concentrations of 100, 200, and 400 μg/μl. Transduction of the mixture of Cas9 enzyme, gRNA, and ssODNs into mouse embryos was performed using the TAKE method (Kaneko et al., 2014; Yoshimi et al., 2016). Briefly, mouse pronuclear-stage embryos were electroporated with Cas9-labelled gRNA and ssODNs using a NEPA21 Super Electroporator (Nepa Gene, Chiba, Japan) with the following conditions: poring pulse: 225 V, 1 ms pulse length, 50 ms pulse interval, 4 pulses, and a 10% decay rate; transfer pulse: 20 V, 50 ms pulse length, 50 ms pulse interval, 5 pulses, and a 40% decay rate. After electroporation, transduction of Cas9 was confirmed using a fluorescence microscope. The embryos that developed into the two-cell stage were selected and transferred into the oviducts of pseudo pregnant female mice. PA-tag insertion into the mouse GPR3 locus by genome editing was confirmed by direct sequencing of the PCR product amplified by the primer sets “GTGCCCATGAATCGTGAGGG” and “GCCATAGAGCTTCCTGCTCC” using DNA extracted from the tails of mice. Homozygous PA-GPR3 transgenic mice were used for immunostaining analysis of GPR3 expression in the retina using an anti-PA antibody.

Immunohistochemical analysis of the mouse retina

For immunohistochemical analysis, mice were transcardially perfused with ice-cold PBS without calcium and magnesium ions followed by a 4% PFA-PBS solution. The eye was then extracted and further fixed with 4% PFA-PBS for 6 h at 4°C. The eye was then immersed in gradually increasing concentrations of sucrose solution (from 10% to 30%) over 3 days and embedded with Tissue-Tek® O.C.T. Compound (Sakura Finetek Japan,

Tokyo, Japan). Coronal sections (14 μm thickness) were obtained using a cryostat (Tissue-Tek Polar DM, Sakura Finetek) and mounted on APS-coated slides (Matsunami, Osaka, Japan). Sections were permeabilized with 0.1%–0.5% Triton-PBS for 1 h at room temperature. After blocking with 3% NGS, the sections were then incubated overnight at 4°C in the following primary antibodies diluted at 1:200 in PBS unless otherwise indicated: anti- βIII Tubulin Monoclonal Antibody (clone TuJ1) (#4466, Cell Signaling Technology, Danvers, MA, USA), anti-GLAST (EAAT1) rabbit monoclonal antibody (#5684, Cell Signaling Technology), anti-Brn3a rabbit polyclonal antibody (ab245230, Abcam, Cambridge, UK), anti-PAX6 rabbit polyclonal antibody (ab5790, Abcam), anti-cAMP rabbit polyclonal antibody (20-198, Sigma-Aldrich), and anti-pERK1/2 antibody (#4370S, Cell Signaling Technology). After serial washes with PBS (-), the sections were then incubated for 1 h at 4°C with the following secondary antibodies diluted at 1:400 in PBS: Alexa488-conjugated goat anti-rabbit (A27034, Thermo Fisher Scientific, Waltham, MA, USA) and Alexa568-conjugated anti-mouse antibody (A11031, Thermo Fisher Scientific) and Alexa647-conjugated goat anti-rabbit antibody (A27040, Thermo Fisher Scientific). After incubation, the sections were washed three times with PBS (-) and embedded using Mowiol anti-fade mounting medium (Merck, Darmstadt, Germany). Fluorescence images were captured using an LSM780 confocal microscope (Zeiss, Oberkochen, Germany).

For immunostaining of flat-mounted retinas, mice were transcardially perfused with ice-cold PBS followed by 4% PFA. The eyes were then enucleated and treated with 4% PFA for an additional hour. After fixation, retinas were frozen in 0.5% Triton-PBS for 15 min at −80°C and then rinsed again in 0.5% Triton-PBS. Frozen-treated retinas were then

incubated with 2% Triton-PBS containing 3% NGS, followed by overnight incubation with an anti-Brn3a rabbit polyclonal antibody (B9684, Sigma Aldrich) diluted 1:100 in 2% Triton-PBS. After serial washes with PBS, the sections were incubated 2 h at 4°C with an Alexa488-conjugated goat anti-rabbit (Thermo Fisher Scientific) secondary antibody diluted 1:400 in PBS. After incubation, the sections were washed with PBS and embedded using Mowiol anti-fade mounting media.

IOP measurement and RGC number evaluation in adult and aged mice

The IOP was measured using a Tono-Lab tonometer (iCare, Vantaa, Finland). The number of RGCs was evaluated in C57BL/6 wild-type and GPR3 knockout mice aged 3–4, 10–12, or 50–60 weeks. The IOP was measured three times in each mouse to obtain the average IOP. Sections from mice subjected to each condition were subjected to Nissl staining with cresyl violet, as previously described (Ikawa et al., 2021), to evaluate the number of RGCs. Images were captured using a BZ-9000 fluorescence microscope (Keyence, Tokyo, Japan) with a 40× oil immersion Nikon Plan Apo VC objective. The number of RGCs was determined in three different locations in each section, and five sections were analyzed in each group. The thickness of the inner plexiform layer (IPL) was also measured within three optic disc diameters from the optic disc using ImageJ/Fiji 1.46 free software (Schneider et al., 2012).

Mouse retinal ischemia/reperfusion (I/R) model and evaluation of the number of RGCs

Retinal I/R was performed according to a previously described protocol (Harada et al., 2000). Briefly, C57BL/6 wild-type and GPR3 knockout mice aged 8–10 weeks were anesthetized with 3.0% isoflurane, and anesthesia was maintained with 1.2% isoflurane in a 2:1 ratio with N_2O/O_2 using a vaporizer (SN-487, Shinano, Tokyo, Japan) and an open face mask. The rectal temperature was monitored and maintained at 37°C using a heating pad and a heating lamp (FHC-HPS; Muromachi Kikai, Tokyo, Japan). Pupil dilation was performed by applying 0.5% tropicamide and 0.5% phenylephrine hydrochloride (Midrin-P, Santen Pharmaceutical, Osaka, Japan) to the conjunctiva. Retinal ischemia was induced by inserting a 33-gauge needle attached to a saline reservoir (0.9% sodium chloride; Otsuka Pharmaceutical, Tokyo, Japan) into the anterior chamber. The reservoir was positioned 135.5 cm higher than the animal, and retinal ischemia was conducted for 40 min. After ischemia was induced, the needle was carefully removed from the anterior chamber, and antibiotics were administered. To evaluate ischemic damage in the retina, the eyes were enucleated 7 days after the operation and then fixed with 4% PFA. The non-treated eye on the contralateral side was analyzed as a normal control. To evaluate the number of RGCs, flat-mounted retinas were stained with anti-Brn3a rabbit polyclonal antibody as described above. Images were captured using an LSM780 confocal microscope (Zeiss). Eight images were obtained from the peripheral and mid-peripheral areas of the four quadrants of each retina. The numbers of total cells in four quadrants of equal area (4.5×10^5 μm^2) were counted and averaged.

Isolation of mouse RGCs and gene transfection

Retinal neuron cultures were prepared from P4 C57BL/6 wild-type mice. After anesthesia, the eyes were enucleated, and retinal cells were dissociated using a papain dissociation system in accordance with the manufacturer's protocols (Worthington Biochemicals, Lakewood, NJ, USA). Dissociated retinal cells were then separated using a two-step gradient method (35%/60% Percoll in PBS; Sigma-Aldrich) for neuronal purification described previously (Tanaka et al., 2007). After centrifugation at 500 × g for 15 min, the fraction enriched with RGCs between the 35% and 60% Percoll layers was collected. Isolated neurons were washed with PBS and then subjected to gene transfection.

For DNA electroporation into RGCs, 5×10^6 dissociated neurons were centrifuged at 800 rpm for 5 min and suspended in 100 μl of Opti-mem (Thermo Fisher Scientific). Then, 3 μg of plasmid DNA was added to the cell suspension for plasmid electroporation. For the RNAi electroporation, 1.5 μg of siRNA and 2 μg of a GFP-expressing plasmid (pMAX-EGFP, Basel, Switzerland) were co-transfected for visualizing transfected cell and neurites. The mixture of transfectant and cells was transferred to a 2 mm gapped cuvette (Nepa Gene). Electroporation was performed using a NEPA21 Super Electroporator (Nepa Gene) under the following conditions: poring pulse: 175 V, 2.5 ms pulse length, 50 ms pulse interval, 4 pulses, and a 10% decay rate; transfer pulse: 20 V, 50 ms pulse length, 50 ms pulse interval, 5 pulses, and a 40% decay rate. After electroporation, the transfected neurons were immediately resuspended in 800 μl of DMEM containing 10% FBS and plated onto poly-L-lysine-coated (1 μg/ml) 12-mm microscope coverslips (Matsunami) at a concentration of $6 \times 10^5/cm^2$. Three to six hours after plating, the culture medium was

replaced with Neurobasal-A medium supplemented with 0.25% GlutaMAX® and 2% B27® supplement (all from Thermo Fisher Scientific).

RNA isolation and real-time PCR

Total RNA was collected from RGCs after culture using an RNeasy Mini Kit according to the manufacturer's protocol (Qiagen, Düsseldorf, Germany). First-strand cDNA was reverse transcribed using a QuantiTect® Reverse Transcription Kit (Qiagen). Specific TaqMan PCR probes for mouse GPR3 and β-actin were used along with predesigned PrimeTime® Standard qPCR assays (IDT). Real-time TaqMan PCR assays were performed using an ABI PRISM® 7500 sequence detection system (Applied Biosystems, Foster City, CA, USA).

Evaluation of neurite outgrowth and neuronal survival in RGCs

To evaluate neurite outgrowth in RGCs, neurons were stained with an anti- βIII Tubulin Monoclonal Antibody (#4466, Cell Signaling Technology) and an Alexa568-conjugated anti-mouse secondary antibody (A11031, Thermo Fisher Scientific). Sections were also counterstained with DAPI (1:10,000 dilution in PBS, Thermo Fisher Scientific). After images were captured using a confocal microscope, the length of the longest neurite process that was positive for both GFP and βIII Tubulin at 24 h and 48 h after transfection was evaluated (at least 60–70 neurons per condition were analyzed) using ImageJ/Fiji 1.46 free software. When evaluating neuronal survival in RGCs, cells with a small nucleus and high DAPI positivity were regarded as apoptotic or dying. The number of apoptotic cells among

all DAPI and βIII Tubulin double-positive cells at 24 h and 48 h after transfection was also determined (at least 60–70 neurons per condition). At least three independent experiments were included in the statistical analysis.

Recombinant adeno-associated virus (rAAV) preparation

The CAG promoter-driven human GPR3 and GFP fusion protein-expressing AAV plasmid (pAAV-GPR3mAGFL; pAAV-GPR3) and control GFP-expressing AAV plasmid (pAAV-mAGFL; pAAV-Mock) were kindly provided by Yoshinaga Saeki. The Rep2-Cap2 plasmid and helper plasmid were obtained from addgene (Watertown, MA, USA). To package the AAV, the pAAV plasmid, Rep2-Cap2 plasmid, and phelper plasmid were co-transfected into HEK293FT cells using a NEPA21 Super Electroporator (Nepa Gene) using the following conditions: poring pulse: 175 V, 2.5 ms pulse length, 50 ms pulse interval, 4 pulses, and a 10% decay rate; transfer pulse; 20 V, 50 ms pulse length, 50 ms pulse interval, 5 pulses, and a 40% decay rate. Packaged AAV vectors were collected from the cells and medium and then concentrated and purified with modified minimal purification methods (Konno and Hirai, 2020). Briefly, the collected medium and cell lysates were filtered with a PES 0.45 μm filter (Merck Millipore, Burlington, MA, USA) to remove cell debris. After filtering, to increase the vector concentration, the composites were applied to a Vivaspin-column (VS2041; Sartorius, Göttingen, Germany) and centrifuged at 8000 rpm for 6–10 h. To evaluate the titers, HEK293 cells were plated in 24-well plates at 2.0×10^5 cells/well 1 day before infection. One microliter of rAAV-Mock or rAAV-GPR3 was diluted in 500 μl of 2% FCS in DMEM culture medium, and then the infection mixture was replaced the following

day. Three days after infection, the cells were fixed, and GFP-positive cells were counted under a BZ-9000 fluorescence microscope (Keyence). Representative images are shown in Suppl.3. The titer of each AAV was determined in triplicate, and five fields per well were counted. The transducing units (TU/ml) were then calculated, and the total number of GFP-positive cells per well was divided by the total volume of the virus in the infection mixture. The following AAV virus titers were used in the current study: rAAV-Mock 10×10^{10} TU/ml and rAAV-GPR3 8×10^{10} TU/ml.

Evaluation of axonal regeneration after ONC

Axonal regeneration was evaluated using a mouse ONC model as previously described with slight modification (Yin et al., 2006). Briefly, male Wild-type and GPR3 knockout mice (6–10 weeks) were anesthetized, and the optic nerve was exposed through a small window via midline incision of the conjunctiva of the left eye. The optic nerve was crushed by pinching with precision forceps (Inami, Tokyo, Japan) at 1 mm from the lamina cribrosa for 10 s under visualization. After the ONC procedure, 1 µl of zymosan (12.5 µg/ml) (Sigma-Aldrich) was carefully intravitreally injected immediately after ONC using a glass micro-pipette inserted posterior to the limbus without injuring the lens. the conjunctiva was sutured, and antibiotics were applied.

To evaluate axonal regeneration, 6-week-old male wild-type mice (C57BL/6) were intravitreally injected 2 weeks prior to ONC with 1 µl of rAAV-Mock or rAAV-GPR3 using a sharp-tipped glass capillary produced using a glass puller (PC-100, Narishige, Tokyo, Japan). To evaluate the combined effect of GPR3 and zymosan, 1 µl of zymosan (12.5

μg/ml) (Sigma-Aldrich) was carefully intravitreally injected immediately after ONC. For the positive control, 1 μl of zymosan (12.5 μg/ml) and 1 μl of CPT-cAMP (50 μM) (Sigma-Aldrich) were simultaneously injected immediately after ONC.

Four weeks after ONC, mice were transcardially perfused with ice-cold PBS followed by 4% PFA, and then the eyes were enucleated. Two days before enucleation, the anterograde tracer Alexa Fluor AM 568 conjugated with the cholera toxin B subunit (Thermo Fisher Scientific) was intravitreally injected to visualize regenerated RGC axons.

The fixed retina was then sagittally sectioned into 14-μm-thick sections using a cryostat, and images were captured using a confocal microscope. To evaluate regenerated axons, the number of regenerated axons was quantified at four different distances: 0–500 μm, 500–1000 μm, 1000–1500 μm, and 1500–2000 μm from the crush site. To evaluate axonal regeneration without zymosan, the number of regenerated axons was quantified at four different distances: 0–100 μm, 100–500 μm, 500–1000 μm, and 1000–1500 μm from the crush site.

Statistical analysis

Statistical analyses were performed using Prism 9 software (GraphPad Software, San Diego, CA, USA). Statistical significance was determined using Student's *t*-test and one-way ANOVA followed by the Bonferroni or Dunnett post hoc test. A value of $p < 0.05$ was considered statistically significant.

Results

GPR3 is highly expressed in mouse RGCs

Although GPR3 is highly expressed in various neurons of the CNS (Ikawa et al., 2020), the expression and distribution of GPR3 in the retina remain unknown. Because a good antibody to detect GPR3 expression in the mice tissue has not been available (Ikawa et al., 2021; Tanaka et al., 2007), we generated PA-tagged GPR3 (PA-GPR3) knockin mice using the CRISPR-Cas9 technique to elucidate the distribution of GPR3 in the retina (Suppl. 1A–B). The immunostaining specificity of an anti-PA antibody for GPR3 was confirmed using PA-tagged GPR3 knockin and wild-type mice (Suppl. 1C–F). A previous report indicated that GPR3 is highly expressed in the medial habenular nucleus. The anti-PA antibody clearly revealed GPR3 expression in the retina and medial habenular nucleus of PA-GPR3 mice, whereas sections from wild-type mice (negative control) did not show prominent staining. Analysis of GPR3 expression using the anti-PA antibody in PA-GPR3 mice revealed relatively high GPR3 expression in the retinal ganglion layer and weak expression in the outer nuclear layer (ONL) and inner nuclear layer (INL) (Fig. 1A–B). GPR3-positive cells in the retinal ganglion layer also expressed βIII Tubulin (Fig. 1C–E) and Brn3a (Fig. 1F–H), which are markers of RGCs. Likewise, GPR3-positive cells in the ONL were partially colocalized with PAX6, an amacrine cell marker (Fig. 1I–K). However, GPR3-positive cells were rarely colocalized with GLAST (Fig. 1L–N), which is a marker of Müller cells. These results suggested that GPR3 expression is relatively high in RGCs but weak in neurons of the ONL and INL and sparse in amacrine cells.

GPR3 knockdown in mice leads to vulnerability of RGCs during aging without affecting IOP and under ischemic conditions

GPR3 expression in neurons may promote survival upon exposure to various apoptosis-inducing stimuli, including ischemia (Tanaka et al., 2014). However, the role of GPR3 in RGC survival remains elusive. To address this issue, we first determined whether GPR3 expression is involved in RGC survival during aging. IPL thickness has been reported to reflect retinal neuron survival in the animal models of retinal ischemia (Harada et al., 2000), we therefore determined RGC survival evaluating both RGC number and IPL thickness. The number of RGCs has been shown to decrease with age. The RGC number remained unchanged until 9 months but gradually decreased via apoptosis from 12 to 18 months in C57/BL6 and DBA/2 mice (Danias et al., 2003). The body weight and IOP were not significantly different between wild-type and GPR3 knockout mice at 8–20 weeks of age (Table 1). Additionally, no difference was observed in the number of RGCs and the IPL thickness between wild-type and GPR3 knockout mice at 3–4 weeks of age (Fig. 2A–C). However, the number of RGCs and the IPL thickness were significantly decreased as early as 10–12 weeks of age in GPR3 knockout mice compared with wild-type mice (Fig. 2A–C). In wild-type mice, the number of RGCs was significantly decreased at 50–60 weeks of age compared with that at 10–12 weeks of age (Fig. 2A–C), which is consistent with previous reports. Furthermore, a reduction in the number of RGCs was also observed in GPR3 knockout mice at 50–60 weeks of age (Fig. 2A–C). These results implied that GPR3 expression in RGCs is related to RGC survival during aging without affecting IOP.

We further explored whether GPR3 expression in RGCs promotes neuronal survival after retinal ischemia. We examined the difference in RGC survival between wild-type and GPR3 knockout mice after retinal I/R. GPR3 expression was significantly decreased as early as 8 h after ischemia and further decreased thereafter until 48 h (Fig. 3A). In the sham operated control group, the number of RGCs and the IPL thickness were significantly reduced in GPR3 knockout mice compared with wild-type mice (Fig. 3B–E). Seven days after the retina was subjected to I/R stress, a similar trend of RGC reduction was observed in wild-type and GPR3 knockout mice (Fig. 3B–E). However, the rates of reduction of the RGC number and IPL thickness were significantly greater in GPR3 knockout mice than those in wild-type mice (Fig. 3F, G). In summary, GPR3 expression in mouse RGCs promotes survival during aging and retinal ischemia.

GPR3 participates in neurite outgrowth and neuronal survival in mouse primary cultured RGCs

We previously reported that GPR3 participates in neurite outgrowth and neuronal survival in CGNs after exposure to various ischemic stimuli (Tanaka et al., 2007; Tanaka et al., 2014). We therefore determined whether GPR3 expression plays a similar role in neurite outgrowth and neuronal survival in RGCs. RGCs exhibited weak GPR3 expression before culturing; however, expression gradually increased until 7 days in culture (Fig. 4A–B), similar to the trend of GPR3 expression in primary cultured CGNs (Tanaka et al., 2007). When GPR3 expression was suppressed in RGCs by siRNA, intrinsic GPR3 expression was significantly reduced compared with that in the control group (Suppl. 2A).

In control siRNA-treated RGCs, the neurite projections increased until 48 h in culture. However, RGC neurites were significantly suppressed at 24 or 48 h in culture when intrinsic GPR3 expression was suppressed by GPR3 siRNA (Fig. 4C–D). Furthermore, RGC survival was significantly reduced in GPR3 siRNA-treated RGCs compared with that in control siRNA-treated RGCs at 24 or 48 h in culture (Fig. 4G–H).

Conversely, when RGCs were transfected with a GPR3-expressing vector, GPR3 expression was significantly increased compared with that in mock vector-transfected RGCs (Suppl. 2B). Neurites in GPR3-expressing vector-transfected RGCs were significantly increased compared with those of mock-transfected cells (Fig. 4E–F). These results indicated that GPR3 expression in cultured RGCs promotes both neurite outgrowth and neuronal survival.

GPR3 expression in RGCs participates in axonal regeneration after ONC

GPR3 expression gradually increased during development in both CGNs and RGCs. However, GPR3 expression is sustained throughout the lifespan in vivo (Ikawa et al., 2021; Tanaka et al., 2009). In neurodegenerative diseases such as Parkinson's disease, neurite retraction, known as "dying-back degeneration", is observed before neuronal cell death (Yaron and Schuldiner, 2016). Interestingly, retraction of RGCs is also observed before RGC death in glaucoma. We then hypothesized that GPR3 may play a role in the maintenance of neurite outgrowth in healthy and pathological conditions. The inflammation-inducing substance zymosan stimulates axonal regeneration, which is further augmented by an increase in intracellular cAMP (Benowitz et al., 2017). Therefore, we

determined whether GPR3 expression in RGCs modulates axonal regeneration after ONC and zymosan treatment. Eyes of wild-type or GPR3 knockout mice were subjected to ONC, and zymosan was intra-orbitally administered immediately after the operation. Axonal regeneration was evaluated by a fluorescent anterograde tracer 28 days after nerve injury. In wild-type mice, axonal regeneration was affected by zymosan (Fig. 5A–B). However, zymosan-mediated axonal regeneration was significantly inhibited in the retinas of GPR3 knockout mice (Fig. 5A–B). These results indicated that GPR3 plays a role in axonal regeneration after ONC when zymosan is administered.

AAV-mediated GPR3 gene transduction in RGCs augmented axon regeneration after ONC

Finally, we determined whether transduction of GPR3 could accelerate axon regeneration after ONC in RGCs. To transduce GPR3 into RGCs, rAAV-mock (GFP-expressing) and rAAV-GPR3 (GFP-tagged GPR3-expressing) plasmids were constructed on the basis of AAV serotype 2 because it preferentially transduces gene delivery in RGCs compared with other cell types in the mouse retina (Park et al., 2008). When rAAV-mock or rAAV-GPR3 was intravitreally injected, GFP was predominantly expressed in RGCs compared with other cell types in the mouse retina (Fig. 6A). Furthermore, in rAAV-GPR3 transfected retinas, the cAMP level and ERK1/2 phosphorylation were increased in RGCs compared with those in rAAV-mock transfected retinas 14 days after transfection (Fig. 6B–C). We then transfected mock or GPR3-exressing AAVs 2 weeks before ONC, and axon regeneration was evaluated 4 weeks after nerve injury using a fluorescence-based

anterograde tracer (Fig. 7A). Axonal regeneration was significantly greater in GPR3-transduced retinas than that in mock-treated retinas (Fig. 7B–C). We further examined GPR3-mediated axonal regeneration after zymosan treatment. Axonal regeneration was enhanced when zymosan was added to mock-treated retinas (Fig. 7D–E). However, axonal regeneration was significantly greater in GPR3-transduced retinas than that in mock-treated retinas after zymosan treatment similar to that observed in cells treated with CPT-cAMP and zymosan (Fig. 7D–E). Axonal regeneration in GPR3-transfected RGCs treated with zymosan was slightly attenuated but similar to that observed in cells treated with CPT-cAMP and zymosan (Fig. 7D–E). These results suggested that GPR3 could accelerate axonal regeneration in mice after axonal injury, especially in combination with zymosan treatment.

Discussion

In the present study, we examined GPR3 expression in mouse RGCs. We found that GPR3 had a neuroprotective effect in aging and ischemic RGCs. Additionally, GPR3 participated in neurite outgrowth and neuronal survival in cultured RGCs. Furthermore, GPR3 expression promoted axonal regeneration and enhanced zymosan-induced axonal regeneration after ONC in mouse RGCs.

GPR3 is expressed in CNS neurons (Ikawa et al., 2021; Saeki et al., 1993; Tanaka et al., 2007), oocytes (Mehlmann et al., 2004), and T lymphocytes (Shiraki et al., 2022). We aimed to clarify the distribution of GPR3 in the retina using a combination of X-gal staining for β-galactosidase and immunostaining as reported previously (Ikawa et al., 2021). However, because strong permeabilization treatment is needed for retinal immunostaining, these staining methods failed to identify the GPR3 distribution in the retina (data not shown). Therefore, we generated PA-tagged GPR3 transgenic mice utilizing the CRISPR-Cas9 genome editing technique (Kaneko et al., 2014; Li et al., 2013; Yoshimi et al., 2016). In the retina, GPR3 was expressed in RGCs and ONL and INL neurons and sparsely expressed in amacrine cells. Therefore, GPR3 expression in the retina showed a similar trend to its expression in CNS neurons. In addition to RGCs, GPR3 expression was also observed in amacrine cells. Amacrine cells are GABAergic inhibitory interneurons that participate in the regulation and integration of activity in bipolar and ganglion cells (Franke and Baden, 2017). Interestingly, our recent report suggested that GPR3 is expressed in basket cells and GABAergic inhibitory interneurons in the cortex, hippocampus, and

cerebellum (Ikawa et al., 2021). However, the function of GPR3 in GABAergic interneurons, including amacrine cells, is still unclear.

In the current study in C57BL/6 mice, we found that GPR3 has a neuroprotective function in RGCs during aging without affecting IOP. Reduction in the number of RGCs with aging is prominent in DBA/2J mice (Danias et al., 2003) and is accompanied by increased IOP and expression of P2X7R in the retina (Pérez de Lara et al., 2019; Turner et al., 2017). The number of RGCs is also slightly decreased via apoptosis from 12 to 18 months of age in C57BL/6 mice (Danias et al., 2003). However, a reduction in the number of RGCs was observed in GPR3 knockout mice as early as 10 to 12 weeks of age despite IOP being normal. The pathogenesis of NTG in humans involves multiple factors, such as systemic hypotension, oxidative stress, glutamate neurotoxicity, vascular dysregulation, and genetic variations (e.g. in optineurin, WD repeat-containing protein 36, and myocilin) (Trivli et al., 2019). In a mouse model of NTG, knockout of the glutamate transporter, GLAST, in Müller glia resulted in RGC degeneration via glutamate accumulation and oxidative stress, which began as early as the neonatal stage (Harada et al., 2007). Furthermore, loss of RGCs was observed in transgenic mice overexpressing mutant optineurin (E50K), reflecting the role of oxidative stress in NTG (Chi et al., 2010). In addition, PAC1, a Gαs-coupled receptor for pituitary adenylate-cyclase-activating polypeptide (PACAP), is expressed in RGCs and amacrine cells (Dénes et al., 2014; Seki et al., 1997), which is similar to the distribution of GPR3 in the retina. Interestingly, knockdown of PAC1 led to a reduction in the number of RGCs, but the IOP in these mice was not reported (Van et al., 2021). These results indicate that, in addition to previously

reported NTG-related genes, GPR3 may also be associated with the age-related degeneration of RGCs and pathophysiology of NTG. However, the molecular mechanism of GPR3-mediated protection during aging and its relationship to the pathophysiology of NTG require further elucidation.

In addition to aging, GPR3 expression in RGCs also has neuroprotective effects after retinal ischemia. Elevation of intracellular cAMP by administration of PACAP or a phosphodiesterase inhibitor has been reported to enhance RGC survival and counteract apoptosis induced by ONC and retinal ischemia via PKA- and CREB-mediated signaling pathways (Cueva Vargas et al., 2016; Seki et al., 2011; Ye et al., 2019). Our previous report also indicated that expression of GPR3 in CGNs promotes neuronal survival after ischemia via PKA, MAPK, and PI3K-dependent signaling in vitro (Tanaka et al., 2014). Therefore, the maintenance of a basal level of cAMP by GPR3 may be tightly linked to neuronal homeostasis during aging and protection against ischemia in GPR3-expressing neurons. Meanwhile, GPR3 expression increases during neuronal differentiation of cultured CGNs and is related to neurite outgrowth and neuronal survival (Tanaka et al., 2007; Tanaka et al., 2021). In cultured RGCs, GPR3 was also involved in the maintenance of RGC survival, and decreased GPR3 expression caused spontaneous neuronal death. Therefore, elevation of GPR3 during neuronal differentiation may participate in both neurite outgrowth and neuronal survival. In various types of neurons, neurite outgrowth and neuronal survival are known to be closely linked to each other and mediated by cAMP-dependent signaling (Boczek et al., 2019). Because GPR3 expression was not only observed during neuronal

development but was also sustained thereafter, GPR3 may participate in both functions throughout life.

Inflammation is the key trigger for axonal regeneration in the retina. The Toll-like receptor 2 ligand zymosan and mechanical injury induce infiltration of immune cells including macrophages, which in turn secrete the EF-hand calcium binding protein oncomodulin, thereby stimulating axonal regeneration (Li et al., 2003; Yin et al., 2006). Neurotrophic factors, such as CNTF or BDNF, combined with lens injury (Müller et al., 2007; Pernet and Di Polo, 2006), and IGF-1 combined with osteopontin (Duan et al., 2015) also participate in axonal regeneration. Importantly, cAMP sensitizes neurons to inflammation-related stimuli or other trophic factors during axonal regeneration (Kurimoto et al., 2013; Kurimoto et al., 2010; Meyer-Franke et al., 1998; Shen et al., 1999; Yin et al., 2006). However, the number of RGCs gradually decreases over time after axonal injury. A loss of responsiveness to peptide trophic factors has been suggested to impede axonal regeneration, and impaired responsiveness is restored by elevation of intracellular cAMP (Shen et al., 1999). Therefore, the decrease in cAMP after nerve injury is the key factor that impairs axonal regeneration after nerve injury. Interestingly, our current study revealed that GPR3 expression decreased following retinal ischemia (Fig. 3A). Moreover, GPR3 knockout mice exhibited limited axonal regeneration, even if zymosan was administered, after retinal injury (Fig. 5A–B). Considering that GPR3 is involved in neuronal survival during aging, GPR3 may maintain a basal level of intracellular cAMP in GPR3-expressing neurons, which is fundamental for preserving neuronal homeostasis, including neuronal survival and axonal regeneration after axonal injury.

In the current study, we found that GPR3 gene transduction into the retina combined with zymosan treatment significantly stimulated axonal regeneration, similar to that observed after administration of the cAMP analog 8-CPT-cAMP combined with zymosan. Elevation of cAMP has a sensitizing effect on growth factors such as CNTF and affects PKA-, ERK-, and PI3K-dependent signaling pathways (Park et al., 2004). Therefore, the sensitizing effect of GPR3 on zymosan observed in the current study may be mediated by signaling downstream of GPR3. Meanwhile, Akt-mediated signaling has diverse effects on axonal regeneration, and downregulation of SOCS3 or PTEN inhibitors can activate PI3K-Akt signaling, thereby augmenting axonal regeneration after ONC (Kurimoto et al., 2010; Park et al., 2004; Park et al., 2009). Furthermore, axon degeneration is regulated by Akt signaling, and enhancement of Akt signaling counteracts retrograde degeneration in dopaminergic axons (Cheng et al., 2011). Moreover, CaMKII-CREB signaling is important for neuronal survival and axon regeneration after ONC (Guo et al., 2021). Therefore, multiple signaling pathways are involved in axonal regeneration of RGCs after injury. Interestingly, GPR3 may activate multiple downstream signaling pathways, such as the cAMP-PKA-CREB, MAPK, and PI3K pathways, when it is expressed in CGNs (Tanaka et al., 2014; Tanaka et al., 2009; Tanaka et al., 2021). Therefore, activation of multiple signaling pathways related to axonal regeneration by GPR3 is a feasible mechanism for axonal regeneration in the retina. In addition, GPR3 can sustain a basal level of cAMP without the addition of a ligand. In the current study, less axonal regeneration was observed in GPR3 transduced cells than in those administered CPT-cAMP combined with zymosan

treatment at 4 weeks after ONC. However, the long-term effect of GPR3 on axonal regeneration beyond 4 weeks after ONC is still unknown.

In the pathogenesis of glaucoma, axonal dysfunction and dying-back degeneration occur before neuronal death (Buckingham et al., 2008; Yaron and Schuldiner, 2016). Axonal transport-related proteins are involved in dying-back degeneration; however, the mechanisms, especially those related to glaucoma, remain unclear. Although downregulation of GPR3 is observed following retinal ischemia, the change in GPR3 expression in RGCs following glaucoma development is still unknown. Clarifying the involvement of GPR3 in axonal degeneration and regeneration may improve the understanding of the pathophysiology of neurodegenerative diseases including glaucoma.

Conflict of Interests: The authors have no conflicts of interest to declare.

Acknowledgments: We wish to thank the Radiation Research Center for Frontier Science and the Natural Science Center for Basic Research and Development, Hiroshima University for the use of their facilities. We also wish to thank Dr. Ji-Ae Ko (Department of Ophthalmology), Graduate School of Biomedical and Health Sciences, Hiroshima University and Dr. Yasuhiko Hayakawa, Nepa Gene Co. Ltd for technical advice.

Funding: This work was supported by a Ministry of Education, Science, Sports and Culture Grant-in-Aid for Scientific Research (to S.T.) and was supported in part by the Japanese Smoking Research Foundation (to S.T.).

References

Benowitz, L. I., et al., 2017. Reaching the brain: Advances in optic nerve regeneration. Exp Neurol. 287, 365-373.

Boczek, T., et al., 2019. Regulation of Neuronal Survival and Axon Growth by a Perinuclear cAMP Compartment. J Neurosci. 39, 5466-5480.

Bonne, C., et al., 1998. Free radicals in retinal ischemia. Gen Pharmacol. 30, 275-80.

Buckingham, B. P., et al., 2008. Progressive ganglion cell degeneration precedes neuronal loss in a mouse model of glaucoma. J Neurosci. 28, 2735-44.

Cavet, M. E., et al., 2014. Nitric oxide (NO): an emerging target for the treatment of glaucoma. Invest Ophthalmol Vis Sci. 55, 5005-15.

Cheng, H. C., et al., 2011. Akt suppresses retrograde degeneration of dopaminergic axons by inhibition of macroautophagy. J Neurosci. 31, 2125-35.

Chi, Z. L., et al., 2010. Overexpression of optineurin E50K disrupts Rab8 interaction and leads to a progressive retinal degeneration in mice. Hum Mol Genet. 19, 2606-15.

Cueva Vargas, J. L., et al., 2016. The glial cell modulator ibudilast attenuates neuroinflammation and enhances retinal ganglion cell viability in glaucoma through protein kinase A signaling. Neurobiol Dis. 93, 156-71.

Cui, Q., et al., 2003. Intraocular elevation of cyclic AMP potentiates ciliary neurotrophic factor-induced regeneration of adult rat retinal ganglion cell axons. Mol Cell Neurosci. 22, 49-61.

Danias, J., et al., 2003. Quantitative analysis of retinal ganglion cell (RGC) loss in aging DBA/2NNia glaucomatous mice: comparison with RGC loss in aging C57/BL6 mice. Invest Ophthalmol Vis Sci. 44, 5151-62.

Dénes, V., et al., 2014. PAC1-expressing structures of neural retina alter their PAC1 isoform splicing during postnatal development. Cell Tissue Res. 355, 279-88.

Duan, X., et al., 2015. Subtype-specific regeneration of retinal ganglion cells following axotomy: effects of osteopontin and mTOR signaling. Neuron. 85, 1244-56.

Eggerickx, D., et al., 1995. Molecular cloning of an orphan G-protein-coupled receptor that constitutively activates adenylate cyclase. Biochem J. 309 (Pt 3), 837-43.

Finkbeiner, S., Greenberg, M. E., 1998. Ca2+ channel-regulated neuronal gene expression. J Neurobiol. 37, 171-89.

Franke, K., Baden, T., 2017. General features of inhibition in the inner retina. J Physiol. 595, 5507-5515.

Gao, Y., et al., 2003. Neurotrophins elevate cAMP to reach a threshold required to overcome inhibition by MAG through extracellular signal-regulated kinase-dependent inhibition of phosphodiesterase. J Neurosci. 23, 11770-7.
Gherghel, D., et al., 2013. Reduction in blood glutathione levels occurs similarly in patients with primary-open angle or normal tension glaucoma. Invest Ophthalmol Vis Sci. 54, 3333-9.
Guo, X., et al., 2021. Preservation of vision after CaMKII-mediated protection of retinal ganglion cells. Cell. 184, 4299-4314.e12.
Gupta, V., et al., 2014. BDNF impairment is associated with age-related changes in the inner retina and exacerbates experimental glaucoma. Biochim Biophys Acta. 1842, 1567-78.
Harada, C., et al., 2000. N-acetylated-alpha-linked-acidic dipeptidase inhibitor has a neuroprotective effect on mouse retinal ganglion cells after pressure-induced ischemia. Neurosci Lett. 292, 134-6.
Harada, T., et al., 2007. The potential role of glutamate transporters in the pathogenesis of normal tension glaucoma. J Clin Invest. 117, 1763-70.
Ikawa, F., et al., 2021. Detailed neuronal distribution of GPR3 and its co-expression with EF-hand calcium-binding proteins in the mouse central nervous system. Brain Res. 1750, 147166.
Kaneko, T., et al., 2014. Simple knockout by electroporation of engineered endonucleases into intact rat embryos. Sci Rep. 4, 6382.
Kao, H. T., et al., 2002. A protein kinase A-dependent molecular switch in synapsins regulates neurite outgrowth. Nat Neurosci. 5, 431-7.
Konno, A., Hirai, H., 2020. Efficient whole brain transduction by systemic infusion of minimally purified AAV-PHP.eB. J Neurosci Methods. 346, 108914.
Kurimoto, T., et al., 2013. Neutrophils express oncomodulin and promote optic nerve regeneration. J Neurosci. 33, 14816-24.
Kurimoto, T., et al., 2010. Long-distance axon regeneration in the mature optic nerve: contributions of oncomodulin, cAMP, and pten gene deletion. J Neurosci. 30, 15654-63.
Lambuk, L., et al., 2022. Brain-Derived Neurotrophic Factor-Mediated Neuroprotection in Glaucoma: A Review of Current State of the Art. Front Pharmacol. 13, 875662.
Lazzara, F., et al., 2021. 1 α,25-dihydroxyvitamin D(3) protects retinal ganglion cells in glaucomatous mice. J Neuroinflammation. 18, 206.
Li, D., et al., 2013. Heritable gene targeting in the mouse and rat using a CRISPR-Cas system. Nat Biotechnol. 31, 681-3.

Li, Y., et al., 2003. Axon regeneration in goldfish and rat retinal ganglion cells: differential responsiveness to carbohydrates and cAMP. J Neurosci. 23, 7830-8.
Luu, J., Palczewski, K., 2018. Human aging and disease: Lessons from age-related macular degeneration. Proc Natl Acad Sci U S A. 115, 2866-2872.
Müller, A., et al., 2007. Astrocyte-derived CNTF switches mature RGCs to a regenerative state following inflammatory stimulation. Brain. 130, 3308-20.
Mallick, J., et al., 2016. Update on Normal Tension Glaucoma. J Ophthalmic Vis Res. 11, 204-8.
Mehlmann, L. M., et al., 2004. The Gs-linked receptor GPR3 maintains meiotic arrest in mammalian oocytes. Science. 306, 1947-50.
Meyer-Franke, A., et al., 1998. Depolarization and cAMP elevation rapidly recruit TrkB to the plasma membrane of CNS neurons. Neuron. 21, 681-93.
Park, K., et al., 2004. Cellular mechanisms associated with spontaneous and ciliary neurotrophic factor-cAMP-induced survival and axonal regeneration of adult retinal ganglion cells. J Neurosci. 24, 10806-15.
Park, K. K., et al., 2009. Cytokine-induced SOCS expression is inhibited by cAMP analogue: impact on regeneration in injured retina. Mol Cell Neurosci. 41, 313-24.
Park, K. K., et al., 2008. Promoting axon regeneration in the adult CNS by modulation of the PTEN/mTOR pathway. Science. 322, 963-6.
Pérez de Lara, M. J., et al., 2019. Potential role of P2X7 receptor in neurodegenerative processes in a murine model of glaucoma. Brain Res Bull. 150, 61-74.
Pernet, V., Di Polo, A., 2006. Synergistic action of brain-derived neurotrophic factor and lens injury promotes retinal ganglion cell survival, but leads to optic nerve dystrophy in vivo. Brain. 129, 1014-26.
Platania, C. B. M., et al., 2022. The P2X7 receptor as a new pharmacological target for retinal diseases. Biochem Pharmacol. 198, 114942.
Promelle, V., et al., 2016. Ocular blood flow and cerebrospinal fluid pressure in glaucoma. Acta Radiol Open. 5, 2058460115624275.
Quigley, H. A., 2011. Glaucoma. Lancet. 377, 1367-77.
Romano, G. L., et al., 2020. P2X7 receptor antagonism preserves retinal ganglion cells in glaucomatous mice. Biochem Pharmacol. 180, 114199.
Saeki, Y., et al., 1993. Molecular cloning of a novel putative G protein-coupled receptor (GPCR21) which is expressed predominantly in mouse central nervous system. FEBS Lett. 336, 317-22.

Schneider, C. A., et al., 2012. NIH Image to ImageJ: 25 years of image analysis. Nat Methods. 9, 671-5.
Seki, M., Lipton, S. A., 2008. Targeting excitotoxic/free radical signaling pathways for therapeutic intervention in glaucoma. Prog Brain Res. 173, 495-510.
Seki, T., et al., 2011. Suppression of rat retinal ganglion cell death by PACAP following transient ischemia induced by high intraocular pressure. J Mol Neurosci. 43, 30-4.
Seki, T., et al., 1997. Distribution and ultrastructural localization of a receptor for pituitary adenylate cyclase activating polypeptide and its mRNA in the rat retina. Neurosci Lett. 238, 127-30.
Shen, S., et al., 1999. Retinal ganglion cells lose trophic responsiveness after axotomy. Neuron. 23, 285-95.
Shiraki, H., et al., 2022. Potential role of inducible GPR3 expression under stimulated T cell conditions. J Pharmacol Sci. 148, 307-314.
Stiles, T. L., et al., 2014. The role of soluble adenylyl cyclase in neurite outgrowth. Biochim Biophys Acta. 1842, 2561-8.
Sveidahl Johansen, O., et al., 2021. Lipolysis drives expression of the constitutively active receptor GPR3 to induce adipose thermogenesis. Cell. 184, 3502-3518.e33.
Tanaka, S., et al., 2007. Neural expression of G protein-coupled receptors GPR3, GPR6, and GPR12 up-regulates cyclic AMP levels and promotes neurite outgrowth. J Biol Chem. 282, 10506-15.
Tanaka, S., et al., 2014. Developmental expression of GPR3 in rodent cerebellar granule neurons is associated with cell survival and protects neurons from various apoptotic stimuli. Neurobiol Dis. 68, 215-27.
Tanaka, S., et al., 2009. The Gs-linked receptor GPR3 inhibits the proliferation of cerebellar granule cells during postnatal development. PLoS One. 4, e5922.
Tanaka, S., et al., 2021. GPR3 accelerates neurite outgrowth and neuronal polarity formation via PI3 kinase-mediating signaling pathway in cultured primary neurons. Mol Cell Neurosci. 103691.
Tao, X., et al., 1998. Ca2+ influx regulates BDNF transcription by a CREB family transcription factor-dependent mechanism. Neuron. 20, 709-26.
Trivli, A., et al., 2019. Normal-tension glaucoma: Pathogenesis and genetics. Exp Ther Med. 17, 563-574.
Turner, A. J., et al., 2017. DBA/2J mouse model for experimental glaucoma: pitfalls and problems. Clin Exp Ophthalmol. 45, 911-922.

Van, C., et al., 2021. Targeted deletion of PAC1 receptors in retinal neurons enhances neuron loss and axonopathy in a model of multiple sclerosis and optic neuritis. Neurobiol Dis. 160, 105524.

Weinreb, R. N., et al., 2014. The pathophysiology and treatment of glaucoma: a review. Jama. 311, 1901-11.

Weisschuh, N., et al., 2005. Prevalence of myocilin and optineurin sequence variants in German normal tension glaucoma patients. Mol Vis. 11, 284-7.

Weisschuh, N., et al., 2007. Variations in the WDR36 gene in German patients with normal tension glaucoma. Mol Vis. 13, 724-9.

Xie, L., et al., 2021. Chemokine CCL5 promotes robust optic nerve regeneration and mediates many of the effects of CNTF gene therapy. Proc Natl Acad Sci U S A. 118.

Yaron, A., Schuldiner, O., 2016. Common and Divergent Mechanisms in Developmental Neuronal Remodeling and Dying Back Neurodegeneration. Curr Biol. 26, R628-r639.

Ye, D., et al., 2019. PACAP Attenuates Optic Nerve Crush-Induced Retinal Ganglion Cell Apoptosis Via Activation of the CREB-Bcl-2 Pathway. J Mol Neurosci. 68, 475-484.

Yin, Y., et al., 2006. Oncomodulin is a macrophage-derived signal for axon regeneration in retinal ganglion cells. Nat Neurosci. 9, 843-52.

Yoshimi, K., et al., 2016. ssODN-mediated knock-in with CRISPR-Cas for large genomic regions in zygotes. Nat Commun. 7, 10431.

Figure legends

Figure 1. G protein-coupled receptor 3 (GPR3) expression in the mouse retina

(A–B) GPR3 expression was investigated using PA-tagged GPR3 knockin mice (PA-GPR3 mice). Retinal sections were stained with an anti-PA antibody. (A) A representative coronal section stained with an anti-PA antibody is shown. (B) A magnified image of the GPR3-positive area in the retina (enclosed in a dotted square in A) is shown. (C–N) Retinal sections from PA-GPR3 mice were double stained with an anti-PA antibody and an anti-βIII Tubulin antibody (C–E), anti-Brn3a antibody (F–H), anti-PAX6 antibody (I–K), or anti-GLAST antibody (L–N). The insets show magnified images of the dotted squares. Scale bar = 20 μm.

Figure 2. G protein-coupled receptor 3 (GPR3) expression in RGCs has a neuroprotective effect during aging

(A–C) The effect of GPR3 expression on RGC survival during aging was evaluated. (A) Representative Nissl-stained retinal sections from wild-type and knockout mice at 3–4 weeks, 10–12 weeks, and 50–60 weeks of age are shown. Scale bar = 30 μm. (B–C) The number of RGCs (B) and the inner plexiform layer (IPL) thickness (C) were compared in Nissl-stained sections from wild-type and knockout mice at 3–4 weeks, 10–12 weeks, and 50–60 weeks of age. Values indicate the mean ± SEM (n = 6 in each group). Statistical significance was evaluated using one-way ANOVA followed by a *post hoc* Bonferroni test. *, $p < 0.05$; **, $p < 0.01$.

Figure 3. G protein-coupled receptor 3 (GPR3) knockout mice were vulnerable to ischemia/reperfusion (I/R) stress

(A) The change of GPR3 mRNA expression after retinal I/R stress was evaluated by real-time RT-PCR. Wild-type mice were subjected to I/R stress for 1 h, and mRNA was evaluated 8, 24, and 48 h after reperfusion. Values indicate the mean ± SEM (n = 3 in each group). (B–G) Wild-type and GPR3 knockout mice were subjected to I/R stress for 1 h. Seven days after I/R stress, the number of RGCs was evaluated. (B–C) Representative coronal sections with Nissl staining (B) and flat-mounted retinas stained with an anti-Brn3a antibody (C) are shown. Scale bar = 30 μm. (D–G) The number of RGCs (D) and the inner plexiform layer (IPL) thickness (E) were compared between wild-type and GPR3 knockout mice. (F–G) The rates of reduction of the RGC number (F) and IPL thickness (G) after I/R stress were evaluated in each group. Values indicate the mean ± SEM (n = 6 in each group). Statistical significance was evaluated using Student's *t*-test (F–G) or one-way ANOVA followed by a *post hoc* Dunnett test (A) or Bonferroni test (D–E). *, $p < 0.05$; **, $p < 0.01$; ***, $p < 0.001$.

Figure 4. G protein-coupled receptor 3 (GPR3) participates in both neurite outgrowth and neuronal survival in mouse primary cultured RGCs

(A–B) Primary cultured RGCs were prepared from P4 neonatal mice and plated onto poly-L-lysine-coated plates. (A) Retinal neurons were then fixed at 0, 1, 2, 4, and 7 DIV and stained with an anti-βIII Tubulin antibody (green). Representative images from retinal neurons captured by confocal microscopy at different time points are shown. Scale bar =

100 μm. (B) Intrinsic GPR3 expression following culture was evaluated using real-time RT-PCR. The graph shows the results from three independent replicates. Values indicate the mean ± SEM in each group. (C–D) RGCs were transfected with either control siRNA + pMAX-EGFP or GPR3 siRNA + pMAX-EGFP plasmid vectors. Twenty-four and 48 h after transfection, neurons were fixed, and the length of the longest neurite of each GFP-positive neuron was measured. (C) Representative images from mouse retinal neurons in each condition. Scale bar = 10 μm. (D) Neurite lengths were compared between control siRNA- and GPR3siRNA-treated neurons. The graph shows the results from four independent replicates. Values indicate the mean ± SEM in each group. (E–F) RGCs were transfected with either pc-mAGFL (mock) or pc-GPR3mAGFL plasmid vectors. Twenty-four and 48 h after transfection, neurons were fixed, and the length of the longest neurite of each GFP-positive neuron was measured. (E) Representative images from mouse retinal neurons in each condition. Scale bar = 10 μm. (F) Neurite lengths were compared between mock and GPR3-expressing RGCs. The graph shows the results from three independent replicates. Values indicate the mean ± SEM in each group. (G–H) The survival of neurons in culture was assessed by DAPI staining. (G) Representative images from control siRNA- and GPR3 siRNA-transfected RGCs at various time points. Scale bar = 10 μm. (H) The ratio of surviving neurons to the total number of DAPI-stained cells at various time points is shown. All graphs in this figure show the results from four independent replicates. Values indicate the mean ± SEM. Statistical significance was evaluated using one-way ANOVA followed by a *post hoc* Dunnett test (B) or Bonferroni test (D, F, H). *, $p < 0.05$; **, $p < 0.01$; ***, $p < 0.001$.

Figure 5. G protein-coupled receptor 3 (GPR3) is involved in axonal regeneration after optic nerve crush (ONC) under zymosan treatment

(A–B) The effect of GPR3 expression on zymosan-mediated axonal regeneration after ONC was evaluated. Axonal regeneration was evaluated using the anterograde fluorescent tracer Alexa 555 conjugated with the cholera toxin B subunit 28 days after ONC. (A) Representative images of regenerated axons after ONC from wild-type or GPR3 knockout mice after zymosan treatment are shown. Asterisks indicate the ONC site. Scale bar = 100 μm. (B) The number of regenerated axons was evaluated at the indicated distances from the crush site. Values indicate the mean ± SEM (n = 3 in each group). Statistical significance was evaluated using one-way ANOVA followed by a *post hoc* Bonferroni test. *, $p < 0.05$.

Figure 6. Adeno-associated virus (AAV)-mediated G protein-coupled receptor 3 (GPR3) gene transduction in RGCs and its effect on downstream pathways in mice

(A) rAAV-mAGFL (rAAV-mock) or rAAV-GPR3mAGFL (rAAV-GPR3) was administered in the vitreous of the mouse retina. Twelve days after inoculation, the retina was fixed, and fluorescent GFP was evaluated by confocal microscopy. Representative images from rAAV-mock or rAAV-GPR3 transfected retinas stained with an anti-βIII Tubulin antibody are shown. The right insets show magnified images of the dotted squares. Scale bar = 25 μm. (B–C) Intracellular cAMP elevation and ERK1/2 phosphorylation were evaluated in rAAV-mock and rAAV-GPR3 transfected RGCs. Retinal sections from each condition were stained with an anti-cAMP antibody (B) and an anti-pERK1/2 antibody (C) 2 weeks after

AAV transfection. The insets show magnified images of the dotted squares. Scale bar = 50 μm.

Figure 7. G protein-coupled receptor 3 (GPR3) elevation in mouse RGCs augmented axonal regeneration after optic nerve crush (ONC)

(A) The timeline and experimental groups used to examine regeneration after ONC. rAAV-mock or rAAV-GPR3 was administered to the mouse retina 2 weeks before ONC. Four weeks after ONC, optic nerve regeneration was assessed by measuring the fluorescence of the anterograde tracer Alexa555 labeled with the cholera-toxin B subunit, which was injected 2 days before fixation. Zymosan and 8-CPT-cAMP were administered immediately after ONC. (B–C) The effect of GPR3 on axonal regeneration was evaluated. (B) Representative images from mock or GPR3 transfected retinas 4 weeks after ONC are shown. Asterisks indicate the ONC site. Scale bar = 100 μm. (C) The number of regenerated axons was evaluated at the indicated distances from the crush site. Values indicate the mean ± SEM (n = 6–7 in each group). (D–E) The combined effect of GPR3 and zymosan on axonal regeneration was evaluated. (D) Representative images from rAAV-mock + zymosan, rAAV-GPR3 + zymosan, or rAAV-mock + zymosan + CPT-cAMP transfected retinas 4 weeks after ONC are shown. Asterisks indicate the ONC site. Scale bar = 100 μm. (E) The number of regenerated axons was evaluated at the indicated distances from the crush site. Values indicate the mean ± SEM (n = 6–7 in each group). Statistical significance was evaluated using one-way ANOVA followed by a *post hoc* Bonferroni test. **, $p < 0.01$; ***, $p < 0.001$.

Table 1. Intraocular pressure in wild-type and G protein-coupled receptor 3 (GPR3) knockout mice at 8–20 weeks of age

The intraocular pressure and body weight were compared between wild-type and GPR3 knockout mice at 8, 10, 12, and 20 weeks of age. Values indicate the mean ± SEM (n = 6–7 in each group). No significant difference was observed between groups.

Figure

Click here to access/download;Figure;220518 GPR3 and retina fig final3.pdf

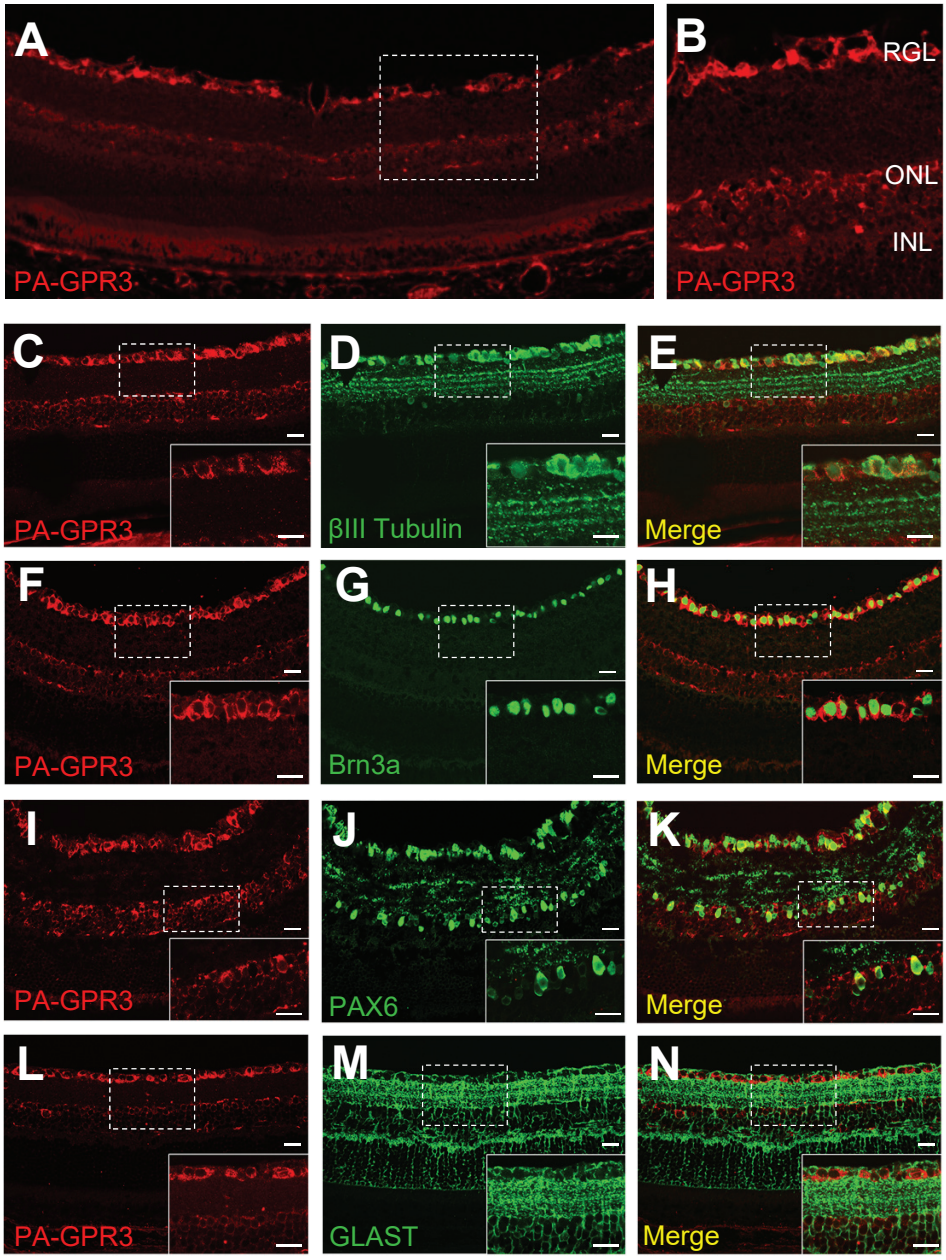

Fig. 1

1.5-column fitting image

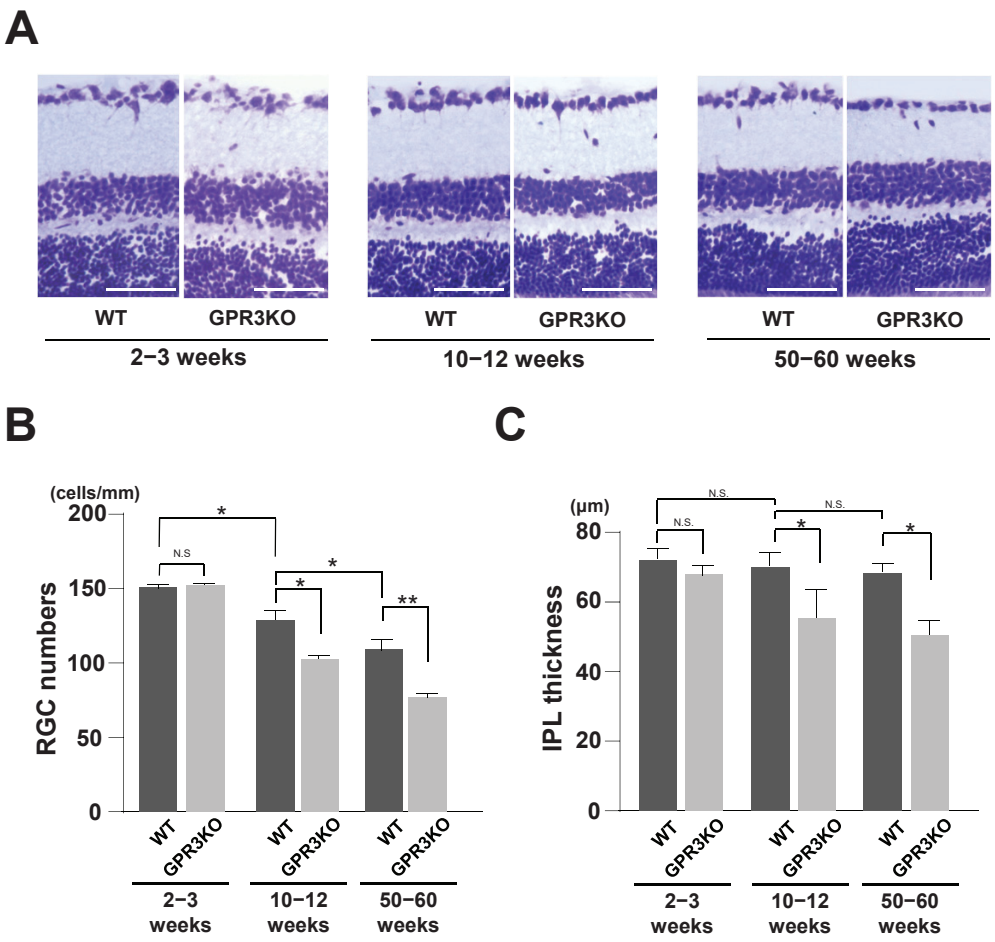

Fig. 2 1.5-column fitting image

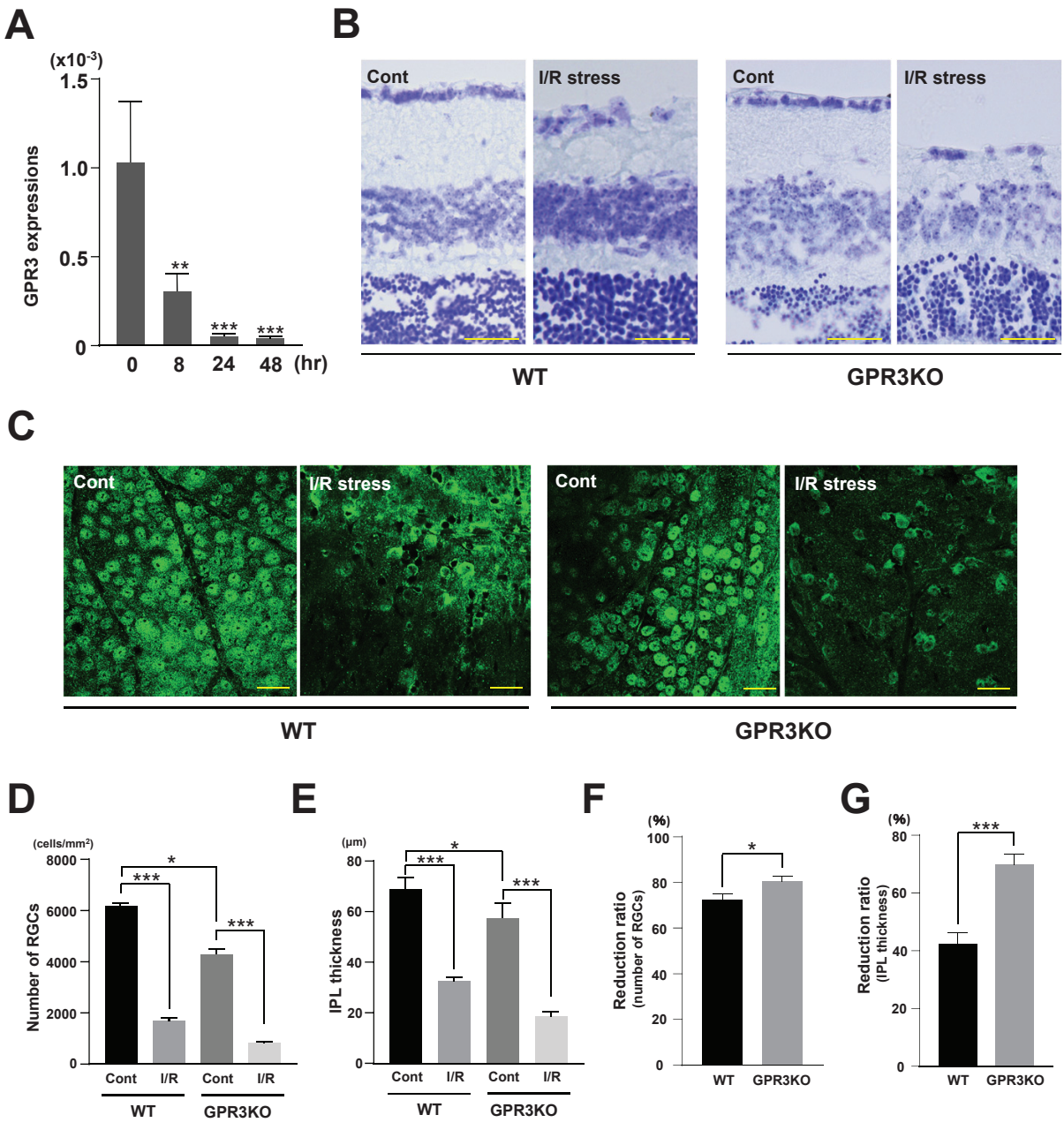

Fig. 3

2-column fitting image

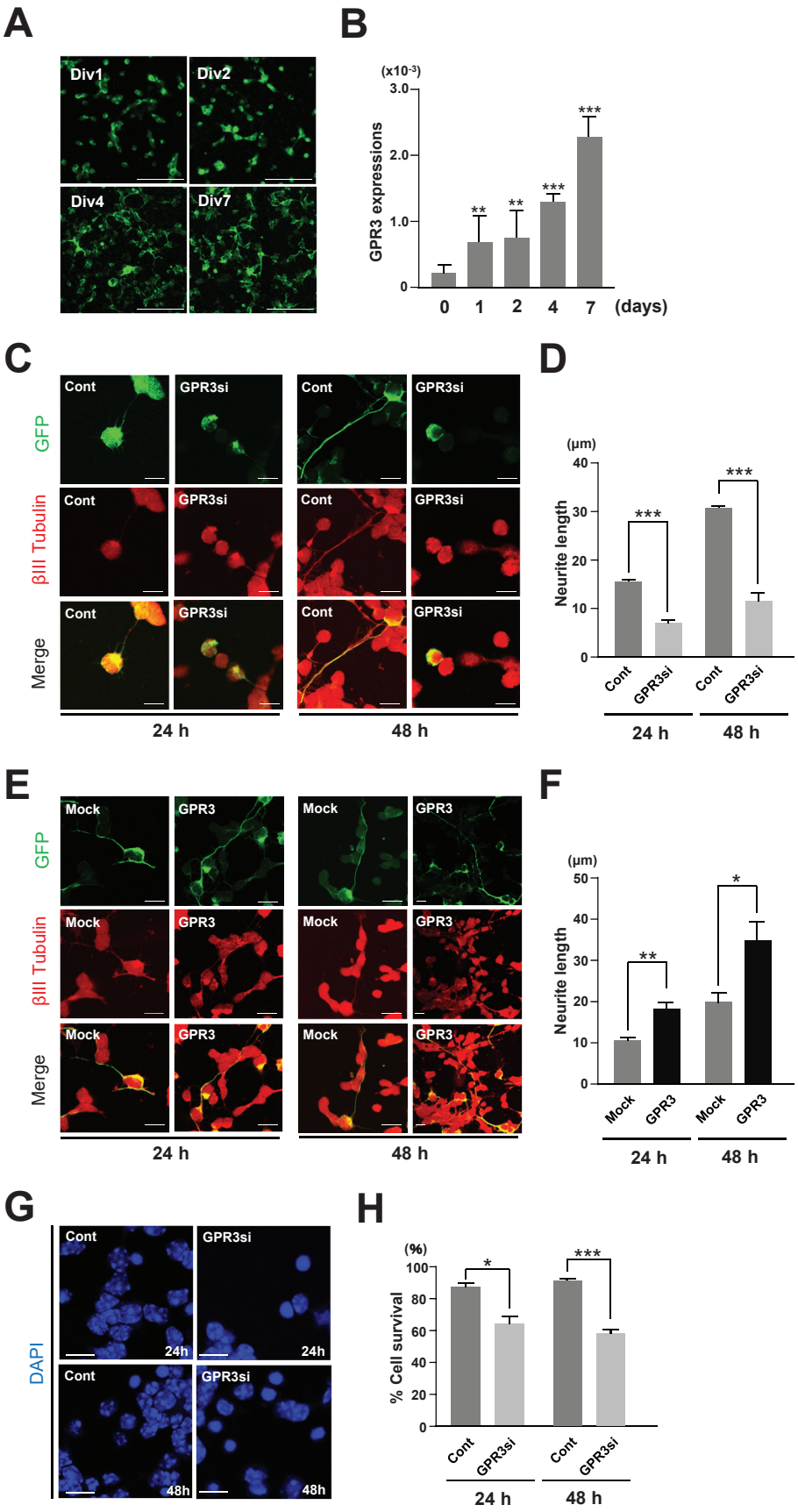

Fig. 4

1.5-column fitting image

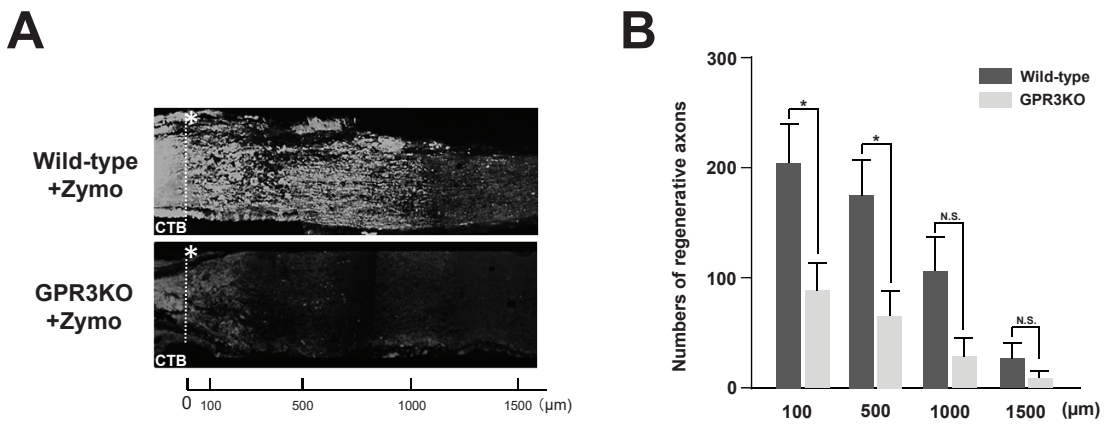

Fig. 5

2-column fitting image

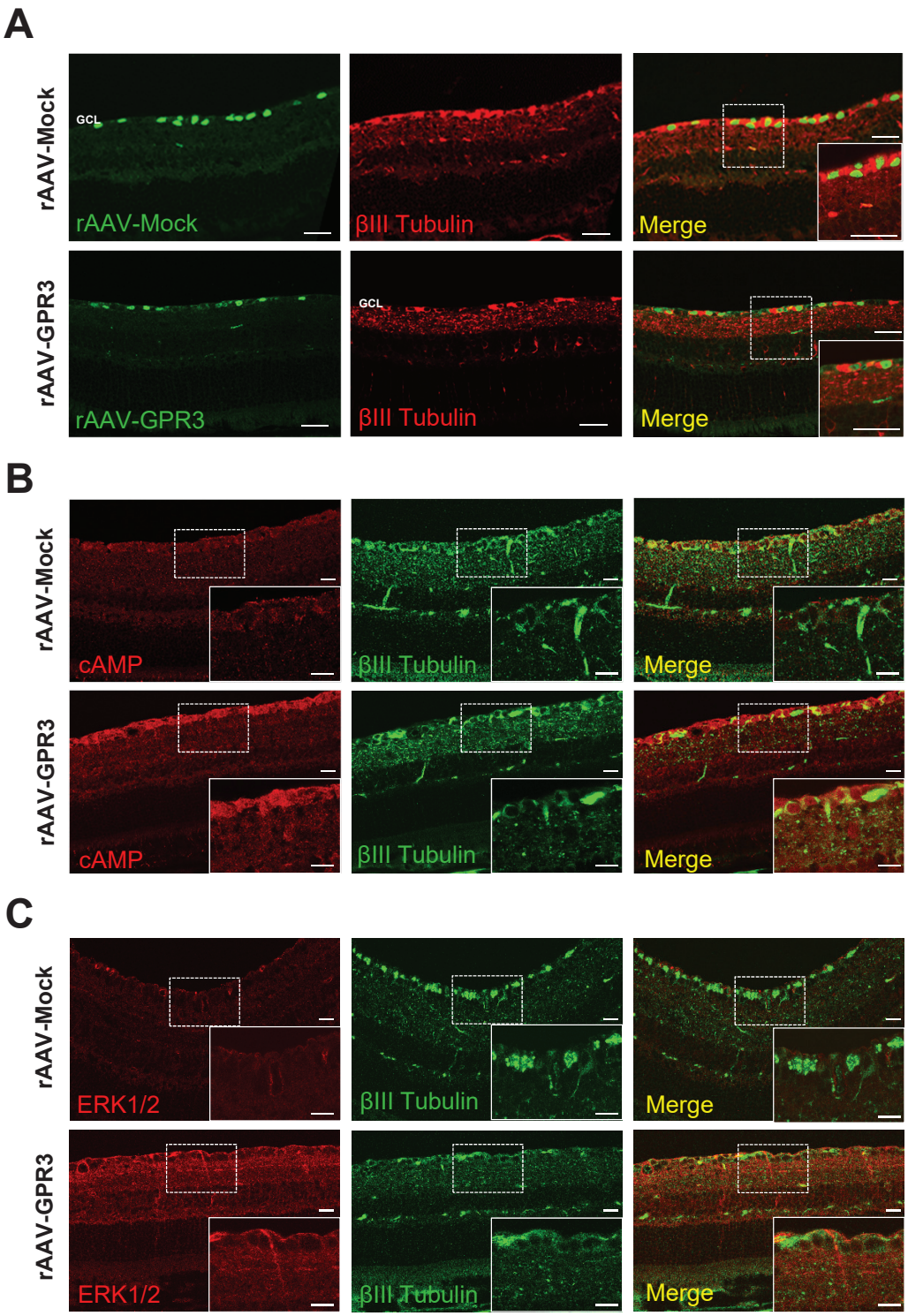

Fig. 6

1.5-column fitting image

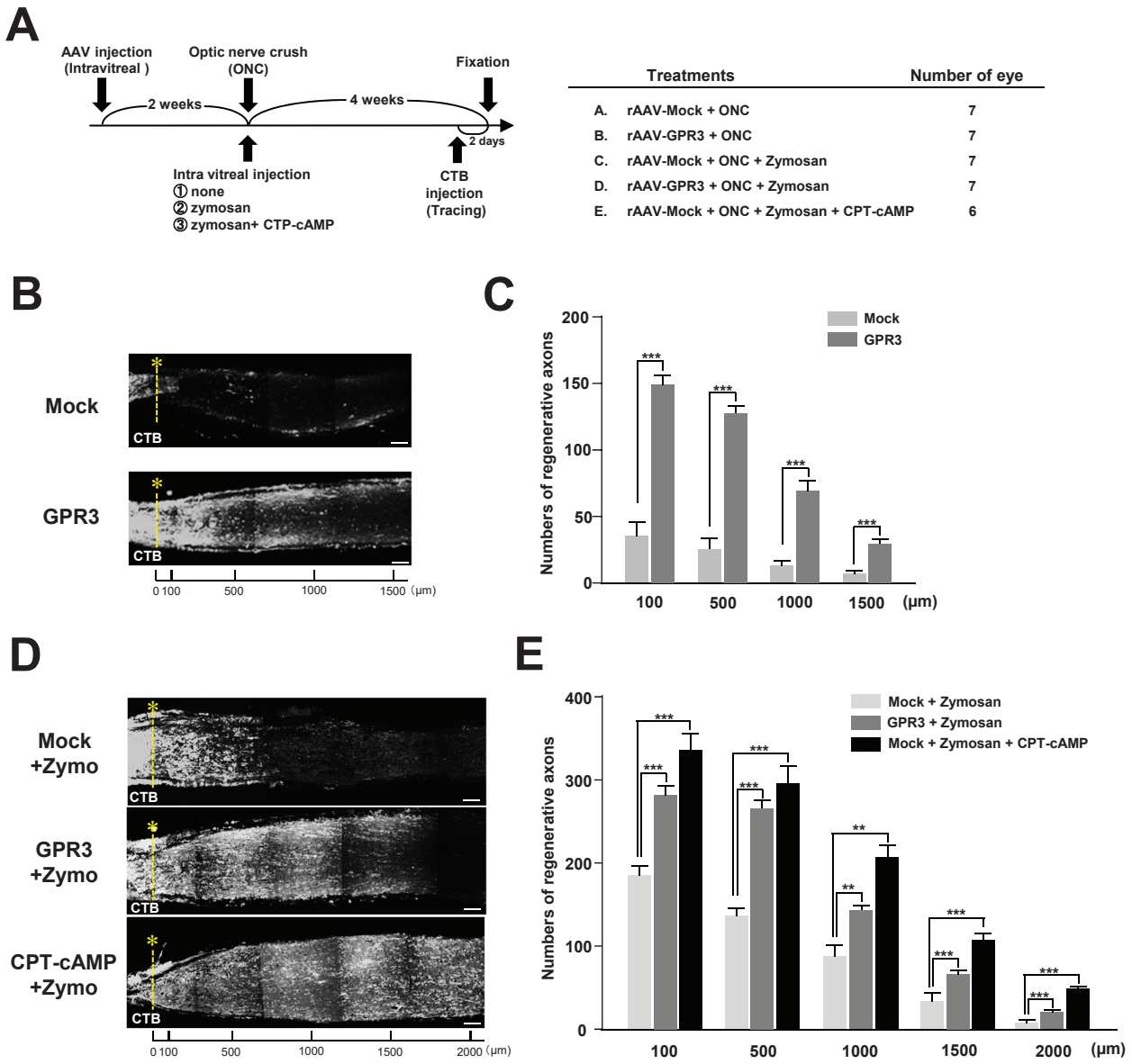

Fig. 7

2-column fitting image

	8 weeks old		10 weeks old		12 weeks old		20 weeks old	
Genotype	**WT**	**GPR3KO**	**WT**	**GPR3KO**	**WT**	**GPR3KO**	**WT**	**GPR3KO**
Body weight (g)	22.5 ± 2.3	21.8 ± 0.6	24.0 ± 0.8	24.4 ± 1.0	24.3 ± 1.5	26.6 ± 1.1	28.9 ± 1.5	30.4 ± 1.8
IOP (mmHg)	13.0 ± 1.5	12.4 ± 0.8	13.7 ± 0.7	12.9 ± 0.9	12.2 ± 0.3	12.6 ± 0.8	11.8 ± 0.62	12.5 ± 0.56

Table. 1